

Impedance Matching of Direct Grid-Connected Renewable Energy Synchronous Generators

1st Dillan Ockhuis
Department of Electrical and
Electronic Engineering
Stellenbosch University
Stellenbosch, South-Africa
d.ockhuis09@gmail.com

2nd Maarten J. Kamper
Department of Electrical and
Electronic Engineering
Stellenbosch University
Stellenbosch, South-Africa
kamper@sun.ac.za

3rd Andrew T. Loubser
Department of Electrical and
Electronic Engineering
Stellenbosch University
Stellenbosch, South-Africa
atloubser@sun.ac.za

Abstract—The connection of synchronous generators directly to renewable energy micro-grids has the advantage of increasing the short circuit strength of the micro-grid. If these generators can also be part of converting renewable energy, such as wind and hydro energy, to electrical power, then it is a further advantage. In this paper the impedance matching of such a directly grid-connected permanent magnet generator, with the grid subjected to power and grid voltage variability, is investigated. It is shown that the optimum reactance for best impedance matching is 0.5 per unit at an optimum induced back electromotive force (EMF) voltage of 1.05 per unit. Additionally, laboratory testing of a direct-grid connected permanent magnet synchronous generator is conducted and its performance evaluated for varying grid voltages and input power conditions.

Index Terms—Synchronous generator, permanent magnet, direct-grid connected, impedance matching, grid voltage variation

I. INTRODUCTION

As the ratio of inverter interfaced renewable energy sources to synchronous generators increases, future power systems may experience reduced short circuit strength due to the lack of rotational inertia present in the system [1], [2] and due to the limited overload capability of inverters (typically between 1.0 and 1.2 pu) [3]. A power system's short circuit ratio (SCR) is commonly used as an indicator of a system's strength and provides an indication of its voltage regulation or "stiffness". When a power system's short circuit strength is insufficient, it becomes more susceptible to voltage instability caused by changes in load and/or faults. This is especially relevant for mini- and/or micro-grids which predominantly comprise of inverter interfaced solar-photovoltaic (PV) arrays and wind turbines which are connected to relatively weak areas of the grid [4]. This is because their control functionality depends, in-part, on a stable grid-reference voltage and phase angle [5]–[7]. The issue of voltage instability is especially relevant for micro-grids operating in islanding mode, when the main grid is no longer available to provide support in terms of the reactive power required to maintain voltage stability [8] or, in the event of a fault, the short-circuit current required to trip the circuit breakers within the micro-grid [9].

Synchronous generators (SGs) and synchronous condensers (SCs) are strong voltage sources capable of supplying relatively large amounts of short circuit current in the event of a grid-fault. Consequently, connecting SGs and/or SCs directly to micro-grids has the advantage of increasing the micro-grid's short circuit strength, as well as improving the system inertia and voltage regulation [10], [11]. Moreover, SGs have been shown to improve the dynamic stability of micro-grids containing PV and inverter-interfaced wind turbines during grid faults and unplanned islanding events [12]. Additionally, SGs have an additional advantage over SCs as they can contribute to power generation within the micro-grid.

An example of a direct-grid connected SG utilizing a renewable energy source is the hybrid excitation synchronous generator (HESG) proposed by [13] for use in small hydropower systems. The HESG consists of two rotors, one of which is a permanent magnet rotor, and the other being a wound rotor. The two rotors share a common stator, which is synchronized with the grid with the help of damper windings. Another example of a direct-grid connected SG utilizing a renewable energy source is the slip-synchronous wind turbine (SS-WT), as shown in Fig. 1. The SS-WT classically consists of fixed-speed turbine blades, a slip-permanent magnetic coupling (S-PMC) and a conventional permanent magnet synchronous generator (PMSG) which is directly connected to the grid [14]. It is the S-PMC which provides the damping to the drivetrain which allows the PMSG to be directly connected to the grid without the need for damper windings or a power electronic converter [14].

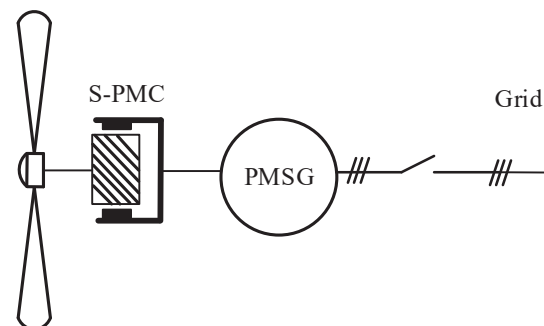


Fig. 1: Example of the SS-PMG wind turbine system where the SG is directly connected to the grid.

However, the fixed-flux nature of directly grid connected PMSG-based wind turbines means that its performance is highly susceptible to grid voltage variations. Furthermore, fixed-speed wind turbine systems have relatively low efficiencies during periods of low wind speed (low-power) as there is no power converter to adjust the turbine's speed to extract the maximum power for a particular wind speed. These issues can be mitigated to some extent by increasing the reactance between the generator and the point of common coupling (PCC). In this paper, the impedance matching of a PMSG with the grid is investigated with the aim of improving the generator's performance during low-power and varying grid voltage conditions. Additionally, the effect of the magnitude of the generator's electromotive force (EMF) on the overall performance is also investigated.

II. MODELLING

The analysis of a SG connected directly to the grid is done on a per unit basis using the equivalent circuit of Fig. 2(a) and the phasor diagram of Fig. 2(b). The input mechanical power, P_{RE} is that of the renewable energy source. As the speed is fixed, we subtract in the analysis a fixed amount of core losses, P_c , from the input power to obtain the developed power, P_d , as

$$P_d = P_{RE} - P_c = E_f I_s \cos(\delta - \theta), \quad (1)$$

where E_f is the induced per unit back EMF due to the permanent magnet (PM) field flux, I_s is the per unit stator current, and δ and θ are the load and power factor angles respectively as explained in Fig. 2(b). Subtracting the conduction losses from the developed power, we obtain the output power, P_s , of the generator supplied to the grid as

$$P_s = P_d - I_s^2 R_s = V_s I_s \cos(\theta), \quad (2)$$

where V_s is the voltage of the ideal micro-grid voltage source as shown in Fig. 2(a). The efficiency of the system is hence determined by

$$\eta = \frac{P_s}{P_s + I_s^2 R_s + P_c} \times 100\%. \quad (3)$$

Between the micro-grid and the back EMF voltages we have the synchronous generator's impedance as

$$Z_s = R_s + jX_s = Z_s \angle \theta_s. \quad (4)$$

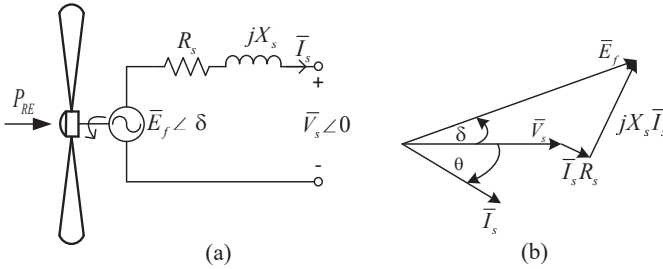


Fig. 2: (a) Synchronous generator equivalent circuit and (b) phasor diagram

The power and reactive power supplied to the grid, P_s and Q_s , can also be expressed as derived in all classical texts by

$$P_s = \frac{V_s E_f}{Z_s} \cos(\theta_s - \delta_s) - \frac{V_s^2}{Z_s} \cos(\theta_s), \text{ per unit watts} \quad (5)$$

and

$$Q_s = \frac{V_s E_f}{Z_s} \sin(\theta_s - \delta_s) - \frac{V_s^2}{Z_s} \sin(\theta_s), \text{ per unit VARs} \quad (6)$$

III. ANALYSIS

The aim of the study is to investigate the effect of the generator's internal impedance, more specifically the synchronous reactance, X_s , and the back EMF voltage, E_f , on the general performance of the generator under variable renewable power and micro-grid voltage conditions. To do this we kept the per unit values of the stator resistance and core losses constant at typical synchronous machine values namely

$$\mathbf{C} = \begin{bmatrix} R_s \\ P_c \end{bmatrix} = \begin{bmatrix} 0.05 \\ 0.02 \end{bmatrix} \text{ pu.} \quad (7)$$

We then determine the generator's performance for a given synchronous reactance, X_s , and a back EMF voltage, E_f , in the ranges of

$$\mathbf{G} = \begin{bmatrix} X_s \\ E_f \end{bmatrix} = \begin{bmatrix} 0.1 < X_s < 1.0 \\ 0.95 < E_f < 1.05 \end{bmatrix} \text{ pu.} \quad (8)$$

The parameters that are then varied for a fixed \mathbf{C} and given \mathbf{G} are the grid supply power and voltage as

$$\mathbf{X} = \begin{bmatrix} P_s \\ V_s \end{bmatrix} = \begin{bmatrix} P_s = 0.2 \text{ and } P_s = 1.0 \\ 0.9 < V_s < 1.1 \end{bmatrix} \text{ pu.} \quad (9)$$

With \mathbf{C} , \mathbf{G} and \mathbf{X} of (7) - (9) known we can determine from (5) the load angle δ as

$$\delta = \theta_s - \cos^{-1} \left[\frac{P_s Z_s}{V_s E_f} + \frac{V_s}{E_f} \cos(\theta_s) \right]. \quad (10)$$

With δ known we can determine Q_s from (6) and the stator current I_s from

$$I_s \angle \theta = \frac{E_f \angle \delta - V_s \angle 0}{Z_s \angle \theta_s}. \quad (11)$$

With all this known we can calculate the efficiency of the generator from (3). The generator's performance parameters that we particularly are interested in are the efficiency η , the reactive power Q_s and the stator current I_s , hence our output vector calculation is

$$\mathbf{Y} = f(\mathbf{X}) = \begin{bmatrix} \eta \\ Q_s \\ I_s \end{bmatrix}. \quad (12)$$

IV. CALCULATED RESULTS

The result of the calculation of \mathbf{Y} of (12) are shown in Figs. 3 and 4 for two parameter values of E_f , namely $E_f = 1.0$ pu and $E_f = 1.05$ pu respectively. From the efficiency results of Figs. 3a and 4a it can be seen that the efficiency at low power drops sharply for small X_s -values, but that good overall results are obtained with $X_s = 0.5$ pu for both values of $E_f = 1.0$ pu and $E_f = 1.05$ pu.

Regarding the reactive power, the overall best result is

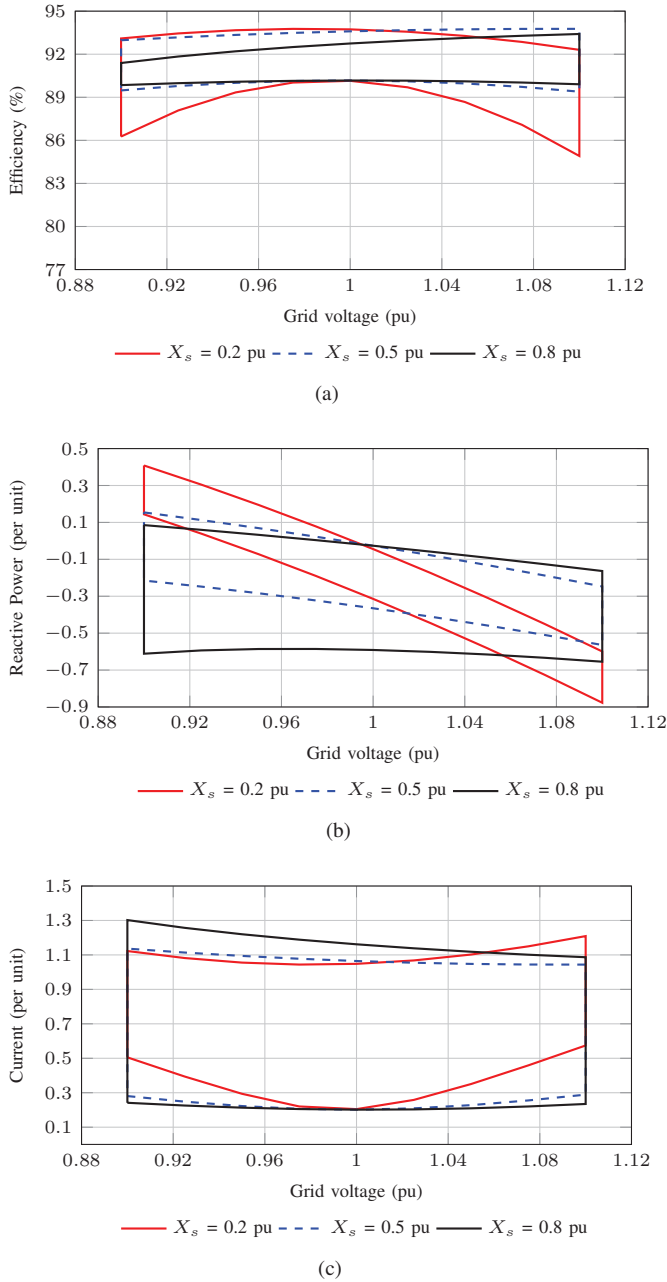


Fig. 3: Efficiency, reactive power and current variance versus supply power and grid voltage with generator reactance X_s a parameter, with $E_f = 1.0$ pu. Note the upper curves are for $P_s = 1.0$ pu and the bottom curves are for $P_s = 0.2$ pu for (a) and (c), whereas for (b), the upper curve is for $P_s = 0.2$ pu and the bottom curve is for $P_s = 1.0$ pu.

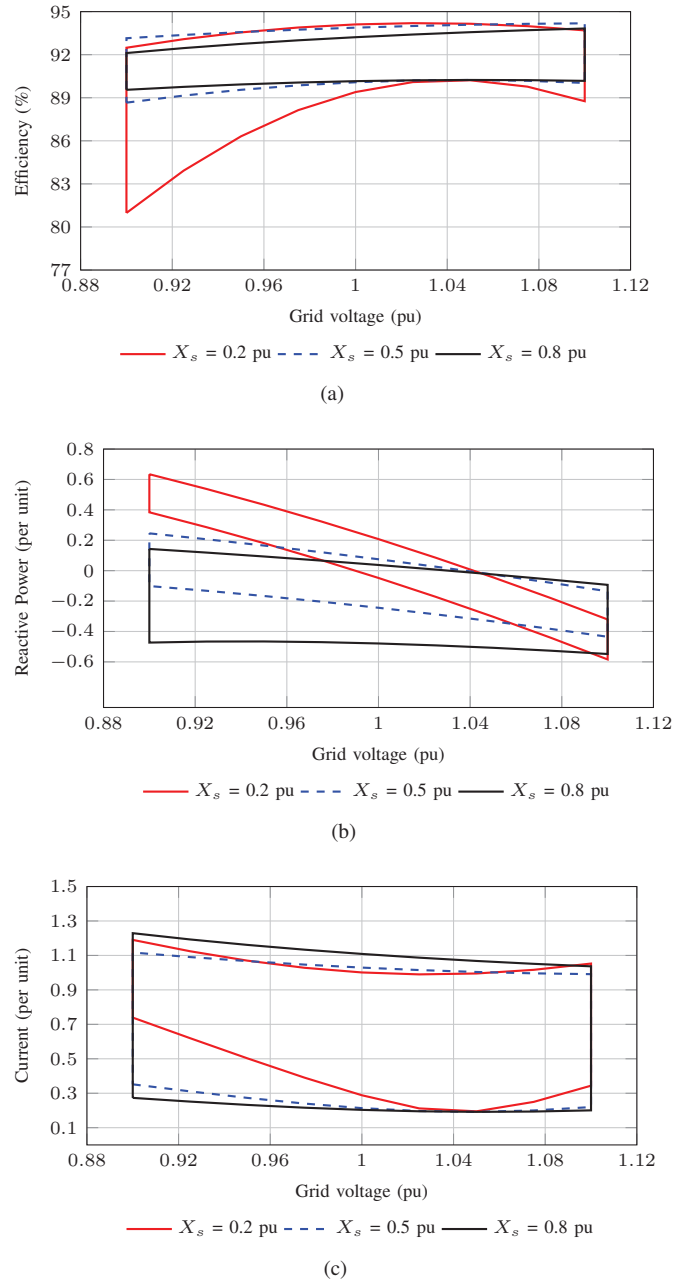


Fig. 4: Efficiency, reactive power and current variance versus supply power and grid voltage with generator reactance X_s a parameter, with $E_f = 1.05$ pu. Note the upper curves are for $P_s = 1.0$ pu and the bottom curves are for $P_s = 0.2$ pu for (a) and (c), whereas for (b), the upper curve is for $P_s = 0.2$ pu and the bottom curve is for $P_s = 1.0$ pu.

obtained with $E_f = 1.05$ pu with X_s either $X_s = 0.2$ pu or $X_s = 0.5$ pu as shown in Fig. 4b.

Regarding the generator current, the best results with the lowest currents and lowest variations are obtained with $E_f = 1.05$ pu and $X_s = 0.5$ pu. One may also consider the case where $X_s = 0.2$ pu, because although the efficiency drops sharply at low voltage and low power as shown in Fig. 4a, the reactive power response of the generator in Fig. 4b is excellent to compensate for low or high micro-grid voltage, precisely

what is needed for grid voltage compensation.

V. MEASURED RESULTS

Fig. 5 shows the laboratory test system layout used to measure the performance of a direct-grid connected slip-synchronous permanent magnet synchronous generator (SS-PMG) under varying grid voltage and varying input power conditions, whereas Fig. 6 shows a simplified line diagram of the test system layout. The SS-PMG is coupled to and driven by an induction motor (IM) which is subjected to speed control by means of an Allen-Bradly *Powerflex 755* variable-speed drive (VSD). The IM-VSD is used to rotate the SS-PMG at synchronous speed and a set of synchronization lights and an oscilloscope are used to connect the generator to the grid once the grid's and generator's respective frequency, voltage-magnitude and voltage-phase angles are aligned. Once grid connected, the voltage at the terminals of the generator is adjusted by means of a variac.

A. Synchronous Generator Parameters

Table I provides some of the specifications of the considered PMSG and Fig. 7 shows the results of an open-circuit test and a short-circuit test conducted to determine its synchronous reactance. From these two tests, the synchronous reactance was determined to be approximately $X_s = 0.17$ pu. From Fig. 7, the PMSG's back EMF voltage, E_f , is approximately 411 V or 1.03 pu, at synchronous speed at 50 Hz.

It should be noted that due to the limitations of the testbench used, the full short-circuit profile of the PMSG could not be measured. Consequently, an external resistance, $R_{ext} = 3.5 \Omega$, was added to the generator's terminals to increase the speed at which rated current occurs.

B. Grid Current versus Grid Voltage

Fig. 8 shows the results of the grid connected test where the grid voltage was varied and the resulting grid current measured

TABLE I: PMSG Specifications.

Parameter	Value	Parameter	Value
Rated voltage, $V_{s(rated)}$	400 V	E_f	1.03 pu
Rated current, $I_{s(rated)}$	21.7 A	Rated power	15 kW
Frequency, f_s	50 Hz	Synchronous speed	150 rpm
X_s	0.17 pu	Number of poles	40
R_s	0.03 pu	Rated torque	1000 Nm

for an input power of 0.2 per unit and 1.0 per unit respectively. Fig. 9 shows the results of another grid connection test where an external inductance of $L_{ext} = 16$ mH was added between the terminals of the generator and the grid. The addition of the external inductance increased the effective reactance between the generator and the grid to $X_s = 0.64$ per unit.

From Figs. 8 and 9, good correlations between the analytical and measured current results are achieved barring a small difference between the results for rated power conditions. The measured results are shown to be in accordance with Fig. 3c and Fig. 4c.

Increasing the effective reactance between the generator and the grid has the effect of decreasing the PMSG's sensitivity to grid voltage conditions. This is especially evident when considering Fig. 9 for low-power conditions where the grid current does not increase above 0.3 per unit at both rated and low grid voltage conditions, keeping the efficiency overall high.

C. Reactive Power versus Grid Voltage

Figs. 10 and 11 show the results of two grid connected tests where the grid voltage is varied and the resulting reactive power is measured for an input power of 0.2 per unit and 1.0 per unit respectively. With reference to Fig. 11, the same external inductance of $L_{ext} = 16$ mH was added between the terminals of the generator and the grid. Once again, good correlations between the analytical and measured results are

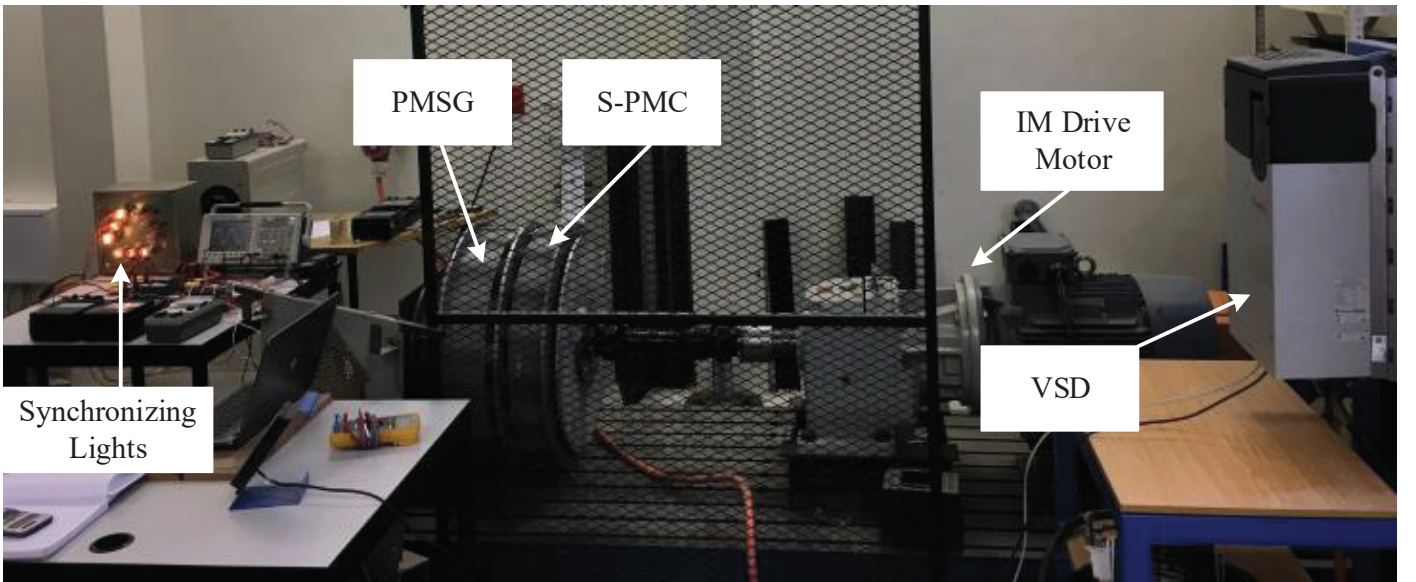


Fig. 5: Test system layout for laboratory measurements of a direct-grid connected 15 kW SS-PMG.

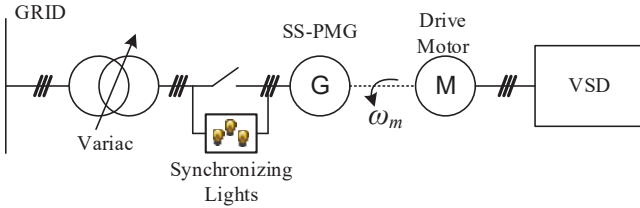


Fig. 6: Simplified line diagram of the grid connected SS-PMG test system.

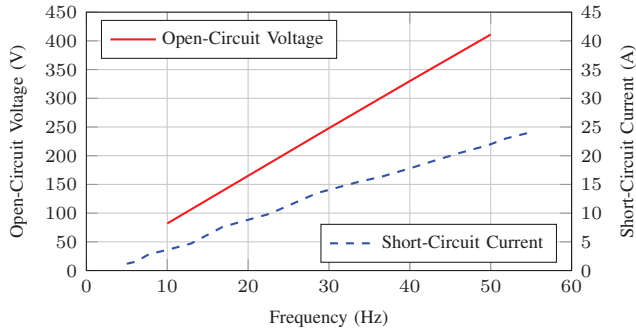


Fig. 7: Results of an open-circuit and short-circuit test conducted on the considered PMSG. An external resistance of 3.5Ω was added to the generator's terminals for the short-circuit test.

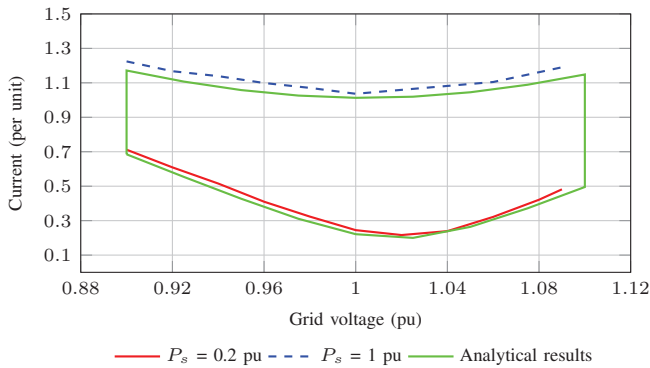


Fig. 8: Measured grid current versus grid voltage with input power as a parameter for a PMSG where, $E_f = 1.03$ pu and $X_s = 0.17$ pu. The analytical results for a SG with $E_f = 1.03$ pu and $X_s = 0.17$ pu are included for comparison.

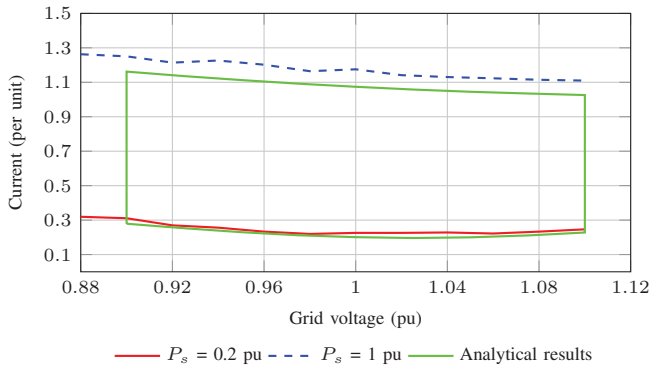


Fig. 9: Measured grid current versus grid voltage with input power as a parameter for a PMSG where, $E_f = 1.03$ pu and $X_s = 0.64$ pu. The analytical results for a SG with $E_f = 1.03$ pu and $X_s = 0.64$ pu are included for comparison.

achieved, barring a slight difference between the results at rated power.

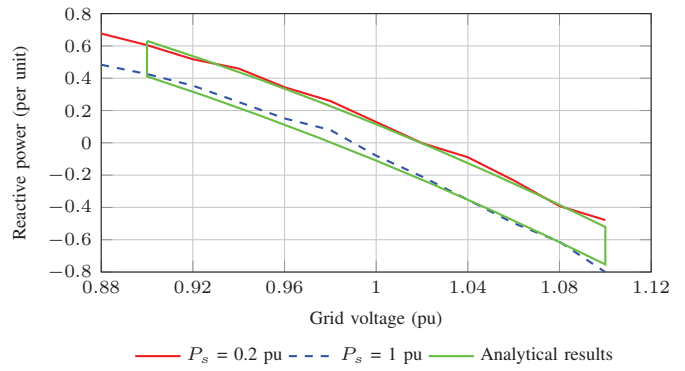


Fig. 10: Measured reactive power versus grid voltage with input power as a parameter for a PMSG where, $E_f = 1.03$ pu and $X_s = 0.17$ pu. The analytical results for a SG with $E_f = 1.03$ pu and $X_s = 0.17$ pu are included for comparison.

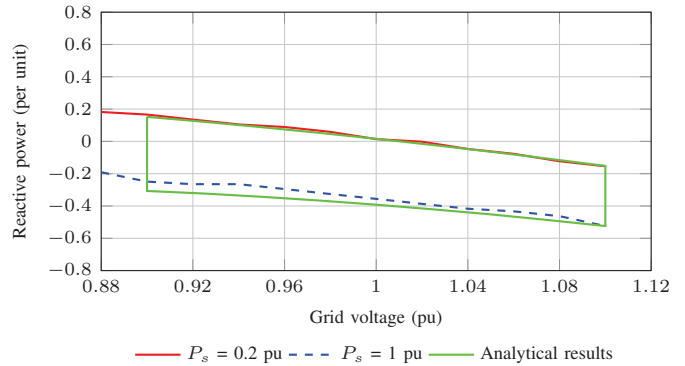


Fig. 11: Measured reactive power versus grid voltage with input power as a parameter for a PMSG where, $E_f = 1.03$ pu and $X_s = 0.64$ pu. The analytical results for a SG with $E_f = 1.03$ pu and $X_s = 0.64$ pu are included for comparison.

With specific reference to Fig. 11, it can be seen that the PMSG operates at near-unity power factor for low-power conditions at a grid voltage of 1.0 per unit. However, there is no condition where the PMSG operates at unity power factor at rated power conditions, as also shown analytically in Fig. 4b.

D. Discussion

With reference to Fig. 10 and 11, it can be seen that the directly grid connected PMSG supplies capacitive reactive power to the grid at low grid voltages and absorbs inductive reactive power during high grid voltages, which implies that it provides "automatic" grid voltage compensation. This form of reactive power compensation is uncontrolled, however, it stands to reason that a directly-grid connected PMSG can aid in assisting grid voltage stabilization by means of supplying or absorbing reactive power in the event of changes in load within a micro-grid, especially during periods of unplanned islanding. Moreover, the classical PMSG can be replaced with a conventional wound-rotor SG or a hybrid-PMSG [13], [15] to provide more control over its reactive power response.

VI. CONCLUSION

In this paper the optimum reactance is investigated for best power matching between the fixed-flux renewable energy PM generator and the micro-grid.

It is shown that the best overall result in terms of efficiency, reactive power and current is obtained with a synchronous reactance of $X_s = 0.5$ pu and a back EMF voltage of $E_f = 1.05$ pu. One could also consider the case with $X_s = 0.2$ pu and $E_f = 1.05$ pu for good reactive power response, but this would result in a lower generator efficiency at low power and low voltage.

Practical testing of a direct-grid connected SS-PMG was conducted to verify the analytical results. It was found that increasing the reactance between the generator and the grid has the effect of decreasing the PMSG's sensitivity towards grid voltage variations.

The outcome of the study allows engineers to design generators according to the required per unit reactance and per unit induced back EMF voltage that will provide the desired performance for a particular micro-grid.

REFERENCES

- [1] A. Gavrilovic, "AC/DC system strength as indicated by short circuit ratios," International Conference on AC and DC Power Transmission, London, UK, 1991, pp. 27-32.
- [2] R. Sharma, M. Singh and D. K. Jain, "Power system stability analysis with large penetration of distributed generation," 2014 6th IEEE Power India International Conference (PIICON), Delhi, 2014, pp. 1-6.
- [3] E. Muljadi, N. Samaan, V. Gevorgian, Jun Li and S. Pasupulati, "Short circuit current contribution for different wind turbine generator types," IEEE PES General Meeting, Providence, RI, 2010, pp. 1-8.
- [4] C. Abbey, B. Khodabakhchian, F. Zhou, S. Denetiere, J. Mahseredjian, G. Joos, "Transient modelling and comparison of wind generator topologies", Proc. International Conference on Power Systems Transients, pp. 1-6, Jun. 2005.
- [5] I. Chung, W. Liu, D. A. Cartes, E. G. Collins and S. Moon, "Control Methods of Inverter-Interfaced Distributed Generators in a Microgrid System," in IEEE Transactions on Industry Applications, vol. 46, no. 3, pp. 1078-1088, May-June 2010.
- [6] A. Singh and B. Singh, "Multifunctional capabilities of converter interfaced distributed resource in grid connected mode," 2012 IEEE 5th India International Conference on Power Electronics (IICPE), Delhi, 2012, pp. 1-6.
- [7] North American Electric Reliability Corporation (NERC), "Integrating Inverter Based Resources into Low Short Circuit Strength Systems," Reliability Guideline, 2017.
- [8] Parol, Mirosław, and Łukasz Rokicki. "Voltage Stability in Low Voltage Microgrids in Aspects of Active and Reactive Power Demand." Archives of Electrical Engineering, vol. 65, no. 1, 1 Mar. 2016, pp. 19-32
- [9] Marnay, Chris, Rubio, F. Javier, and Siddiqui, Afzal S. "Shape of the microgrid". In: Power Engineering Society Winter Meeting, 2001, IEEE, vol. 1. 2001. p. 150-3.
- [10] J. Jia, G. Yang, A. H. Nielsen, E. Muljadi, P. Weinreich-Jensen and V. Gevorgian, "Synchronous Condenser Allocation for Improving System Short Circuit Ratio," 2018 5th International Conference on Electric Power and Energy Conversion Systems (EPECS), Kitakyushu, Japan, 2018, pp. 1-5.
- [11] F. O. Igbinovia, G. Fandi, Z. Müller, J. Švec and J. Tlustý, "Optimal location of the synchronous condenser in electric-power system networks," 2016 17th International Scientific Conference on Electric Power Engineering (EPE), Prague, 2016, pp. 1-6.
- [12] A. V. Jayawardena, L. G. Meegahapola, S. Perera and D. A. Robinson, "Dynamic characteristics of a hybrid microgrid with inverter and non-inverter interfaced renewable energy sources: A case study," 2012 IEEE International Conference on Power System Technology (POWERCON), Auckland, 2012, pp. 1-6.
- [13] K. Kamiev, A. Parviainen and J. Pyrhönen, "Hybrid excitation synchronous generators for small hydropower plants," 2016 XXII International Conference on Electrical Machines (ICEM), Lausanne, 2016, pp. 2529-2535.
- [14] J. H. J. Potgieter and M. J. Kamper, "Design of New Concept Direct Grid-Connected Slip-Synchronous Permanent-Magnet Wind Generator," in IEEE Transactions on Industry Applications, vol. 48, no. 3, pp. 913-922, May-June 2012.
- [15] L. L. Amuhaya and M. J. Kamper, "Design and optimisation of grid compliant variable-flux PM synchronous generator for wind turbine applications," 2015 IEEE Energy Conversion Congress and Exposition (ECCE), Montreal, QC, 2015, pp. 829-836.